



Crack path in a Zn-Cu-Al PE alloy under uniaxial load

Vittorio Di Cocco, Francesco Iacoviello, Luigi Tomassi, A. Rossi

Università di Cassino e del Lazio Meridionale, DiCeM, via G. Di Biasio 43, 03043 Cassino (FR), Italy
v.dicocco@unicas.it

Stefano Natali, Valerio Volpe

Università di Roma "La Sapienza", DICMA, via Eudossiana 18, Rome, Italy

ABSTRACT. Pseudo-elastic (PE) materials are an important class of metallic alloy which exhibit unique features with respect to common engineering metals. Because of these unique properties, PEs are able to recover their original shape after high values of mechanical deformations, by removing the mechanical load (PE). From the microstructural point of view shape memory and pseudo-elastic effects are due to a reversible solid state microstructural diffusionless transitions from austenite to martensite, which can be activated by mechanical and/or thermal loads. Copper-based shape memory alloys are preferred for their good memory properties and low cost of production.

This paper describes the main crack initiation and its propagation in an tensile test in order to evaluate crack path and its behaviour at low and at high values of deformation. Both grain boundary chemical properties and X-ray diffraction will be discussed in order to correlate structural transition involved in an Cu-Zn-Al alloy characterized by a PE behaviour.

SOMMARIO. I materiali a comportamento pseudo-elastico (PE) sono una importante classi di materiali che esibiscono una caratterisitica unica nel panaorama del materiali metallico, cioè quella di recuperare, alla temperatura ambiente, la forma iniziale anche a seguito di deformazioni molto elevate. Ciò è dovuto alla capacità di questi materiali di modificare, in modo completamente reversibile, la struttura cristallina di partenza secondo meccanismi non diffusivi come risposta a sollecitazioni meccaniche esterne. Tali trasformazioni sono completamente reversibili appena viene tolto il carico esterno.

In questo lavoro è stata osservata la nucleazione e la propagazione della cricca principale che ha portato alla rottura di provini di trazione uni assiali in lega di ottone a comportamento PE. I risultati delle analisi micrografiche sono stati correlati alle analisi diffrattometri che X-ray.

KEYWORDS. Zn-Cu-Al alloy; Pseudoelastic behaviour; Crack micromechanisms.

INTRODUCTION

Shape memory alloys (SMA) and pseudo-elastic alloys (PEA) are able to recover their original shape after high mechanical deformations: (SMA's) by heating up to characteristic temperature (Shape Memory Effect, SME), while PEA's recover their shape simply by removing the mechanical load (Pseudo-elastic Effect, PE). Different shape memory alloys have been optimized in the last decades, such as the copper-zinc-aluminum (ZnCuAl), copper-aluminum-nickel (CuAlNi), nickel-manganese-gallium (NiMnGa), nickel-titanium (NiTi), and other SMAs obtained alloying zinc,



copper, gold, iron, etc.. However, the near equiatomic NiTi binary system shows the most interesting properties and it is currently used in an increasing number of applications in many fields of engineering for the realization of smart sensors and actuators, joining devices, hydraulic and pneumatic valves, release/separation systems, consumer applications and commercial gadgets [1, 2]. Due to their good biocompatibility, another important field of SMA application is medicine, where the pseudo-elasticity is mainly exploited for the realization of several components such as cardiovascular stents, embolic protection filters, orthopedic components, orthodontic wires, micro surgical and endoscopic devices [3].

From the microstructural point of view, shape memory and pseudo-elastic effects are due to a reversible solid state microstructural transition from austenite to martensite, which can be activated by mechanical and/or thermal loads [4].

Copper-based shape-memory alloys are very sensitive to thermal effects, and it is possible that in thermal cycles its properties change (e.g., shape-recovery ratio, transformation temperatures, crystal structures, hysteresis and mechanical behavior).

Cu–Zn–Al shape memory alloys exhibit shape memory behavior within a certain range of composition. It is characterized by a stable high temperature disordered bcc structure named β -phase. After a customized cooling process, a B2 structure is obtained followed a DO3 ordering. It is also known that martensite stabilization can be reduced by a step-quenched treatment.

Cu ZnAl alloys mechanical properties are influenced by [5]:

- martensite stabilization;
- grain size;
- processes procedure (e.g., temperature, heat treatment cycles number).

Other investigations carried out on CuZnAl alloys, showed a strain influence on the macroscopic behavior and on martensite morphology. Martensitic transformation occurs initially in deformed material and the manufactured shape follows the transformation [6]. Larger grains dimensions allow an easier transformation process, allowing the growth of 18R martensite [7].

In this work, damaging micromechanism during a tensile test in a CuZnAl alloy was investigated, focusing the crack initiation and its stable growth. Deformation influence on alloy microstructure was investigated during the tensile test by means of X-Ray diffraction.

INVESTIGATED MATERIAL AND EXPERIMENTAL PROCEDURES

In this work a CuZnAl pseudo-elastic alloy, made in the laboratory by using a controlled atmosphere furnace and characterized by chemical composition shown in Tab. 1, was used to investigate mechanical behavior in tensile conditions. Prior to evaluating mechanical properties, a chrono-amperometric tests was performed in order to evaluate the homogeneity of material and its electrochemical behaviours, using a 0.1 mol NaCl solution and a -50mV/SCE for 30, 60, 600, 900, 1800s.

The evolution of the microstructure during uniaxial deformation was analyzed by a miniature testing machine which allows in-situ scanning electron microscopic (SEM) observations as well as X-Ray micro-diffraction analyses.

Cu	Zn	Al	Other
73.00	21.80	5.04	0.16

Table 1: Chemical composition of CuZnAl investigated alloy.

Specifically, the testing machine is equipped with a simple and removable loading frame, which allows SEM and X-Ray analyses at fixed values of applied load and/or deformations. The machine is powered by a stepping motor, which applies the mechanical deformation to the specimen through a calibrated screw, with pitch of 0.8 mm, and a control electronic allows simultaneous measurement and/or control of applied load and stroke of the specimen head. The stroke is measured by a Linear Variable Differential Transformer (LVDT) while the load is measured by two miniaturized load cells with maximum capacity of 10 kN. Miniature dog bone shaped specimens were machined from alloy samples obtained by cold cutting of mini sheets from as cast ingots, by wire electro discharge machining.

Step by step isothermal tensile tests were carried out, at room temperature, at increasing values of the specimens elongation. For each loading step, the loading frame containing the specimen was removed from the testing machine, at fixed values of deformation. The specimens, under load condition, were analyzed by means of:



- 1) a light optical microscope, characterized by a wide observation field; all the investigated specimen's length was observed in order to identify the crack initiation site. The investigated steps are $\epsilon_{\text{eng}} = 0\%$, 5% , 10% , and 14% (failure);
- 2) a diffractometer in order to evaluate XRD spectra. XRD measurements were made with a Philips X-PERT diffractometer equipped with a vertical Bragg–Brentano powder goniometer. A step–scan mode was used in the 2θ range from 40° to 90° with a step width of 0.02° and a counting time of 2 s per step. The employed radiation was monochromated $\text{CuK}\alpha$ (40 kV – 40 mA). The calculation of theoretical diffractograms and the generation of structure models were performed using the PowderCell software [8]. The investigated steps are at $\epsilon_{\text{eng}} = 0\%$ and 5% .

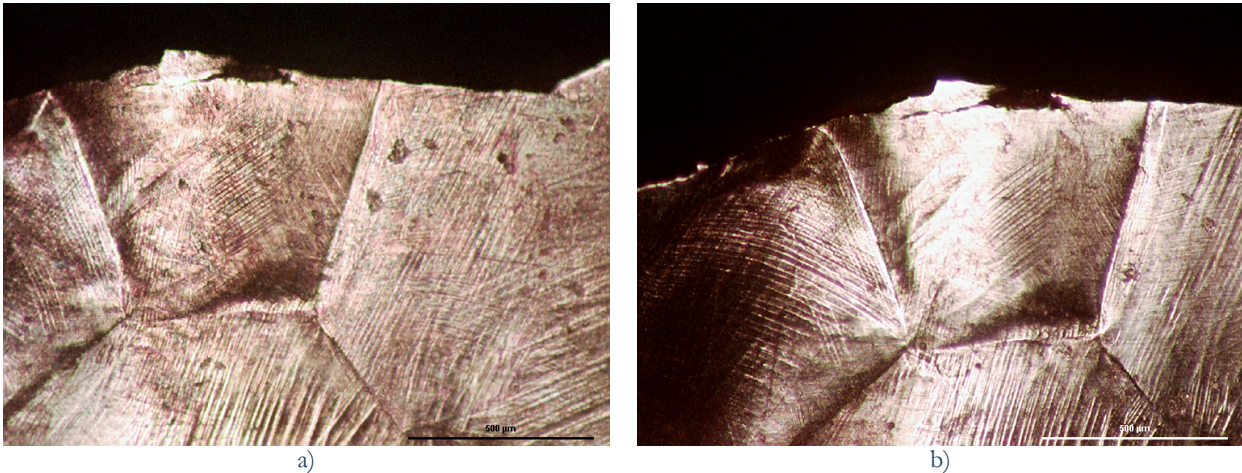


Figure 1: Etched surface: a) etched-deformed and observed, b) deformed, cleaned and re-etched.

Finally, SEM observations on fracture surface have been performed in order to evaluate the main fracture micromechanisms.

In order to check the correctness of the LOM observation procedure, a preliminary test was performed. An unloaded and metallographically prepared specimen was deformed up to $\epsilon_{\text{eng}} = 0\%$ and then LOM observed (Fig. 1a). Subsequently the same specimen (loaded) has been metallographically prepared and LOM observed (Fig. 1b). The possibility to follow the grain modifications in the investigated SMA is possible by performing the first metallographic preparation.

EXPERIMENTAL RESULTS AND COMMENTS

The inhomogeneities of material has been highlighted by crono-amperometric tests which results are shown in Fig. 2. The electrochemical behaviour is characterized by a decrease of current due to a slight passive property, due to the presence of corrosion product formation on the etched surface. But the corrosion products are not homogenous, because the structure appears different between bulk of grains, boundary and a not negligible zone riding on the boundary of grains.

The evolution of etching boundary grains and an “acicular like” zone near boundary grains are readily evident, although at higher value of times, the corrosion goes on the bulk and degenerates (metallography at 1800s in the Fig. 2).

Engineering stress strain curve of investigated alloy is shown in Fig. 3, where a plateau has not been observed. The investigated deformation conditions correspond to:

1. $\epsilon_{\text{eng}} = 0\%$ - starting test conditions;
2. $\epsilon_{\text{eng}} = 5\%$ - near yield point;
3. $\epsilon_{\text{eng}} = 10\%$ - plastic zone;
4. $\epsilon_{\text{eng}} = 14\%$ - specimen failure.

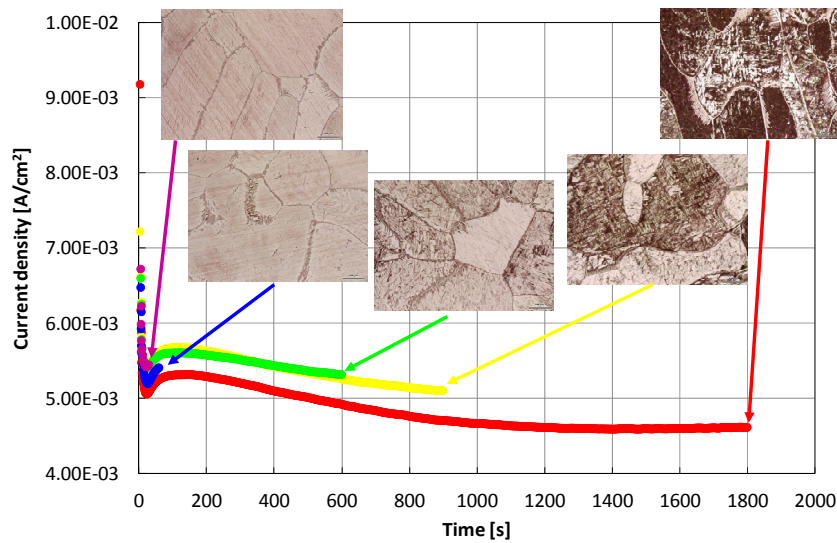


Figure 2: Electrochemical behavior and microstructure etched of material.

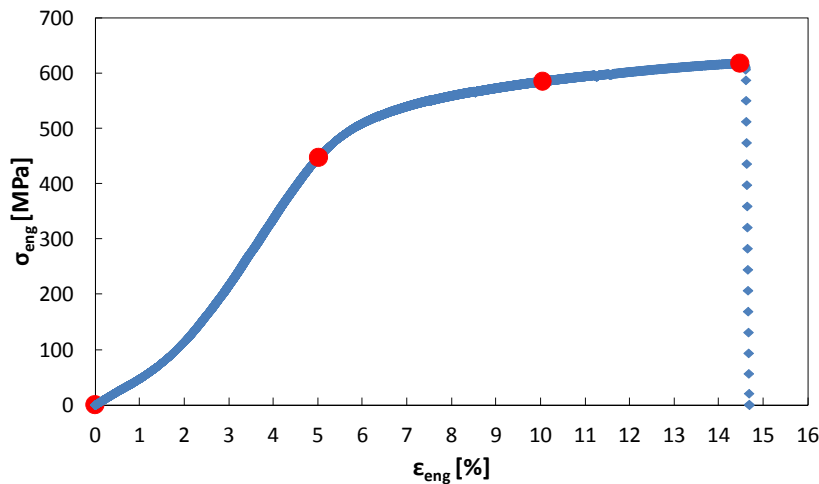


Figure 3: Engineering Stress-Strain curve (red points correspond to the investigated conditions).

The failure initiation site (Fig. 4), for $\epsilon_{eng} = 0\%$, is characterized by the presence of three grains (Fig. 4a). For $\epsilon_{eng} = 5\%$ (Fig. 4b) the three grains show an unchanged orientation, no sub-grains nucleation and a grain boundary deformation from linear to curved shape, probably due to phase transition. This is more evident in the grain on the left, where a surface modification is observed (sort of zig-zag lines on the surface). For $\epsilon_{eng} = 10\%$ (Fig. 4c), an intergranular crack initiate from the lateral specimen surface, with a secondary intergranular crack, that is more or less parallel to the applied load. This secondary crack is probably due to the transition of phases in grains with different orientations, together with a consequent τ stress increase at the grain boundary [7]. The increase of the macroscopical deformation implies an increase of the localized damage level, with the coalescence of main and secondary cracks (Fig. 4d). Final failure is obtained by means of a crack propagation from one side to the opposite side of the specimen (“fracture ending zone”).

In Fig. 5, the “fracture ending zone” is shown. For $\epsilon_{eng} = 0, 5$ and 10% , corresponding respectively to Fig. 5a, b and c, no transformations are evident: surface modifications due to phase transformations are not observed in this zone. For $\epsilon_{eng} = 14\%$ (Fig. 5d), it is possible to observe a localized ductile deformation.

Evidence of structure transitions are in Fig. 6, where two diffractograms show respectively the undeformed and the deformed at $\epsilon_{eng} = 5\%$ specimen. The undeformed specimen spectrum shows four peaks corresponding to $42.35^\circ, 43.71^\circ, 70.39^\circ, 80.23^\circ$. The $\epsilon_{eng} = 5\%$ deformed specimen shows also four peaks but corresponding to different diffraction angles ($42.27^\circ, 43.43^\circ, 43.85^\circ$ and 85.71°). Peaks modifications (considering both angles and intensity) show the mechanical deformation influence on the microstructure modifications.

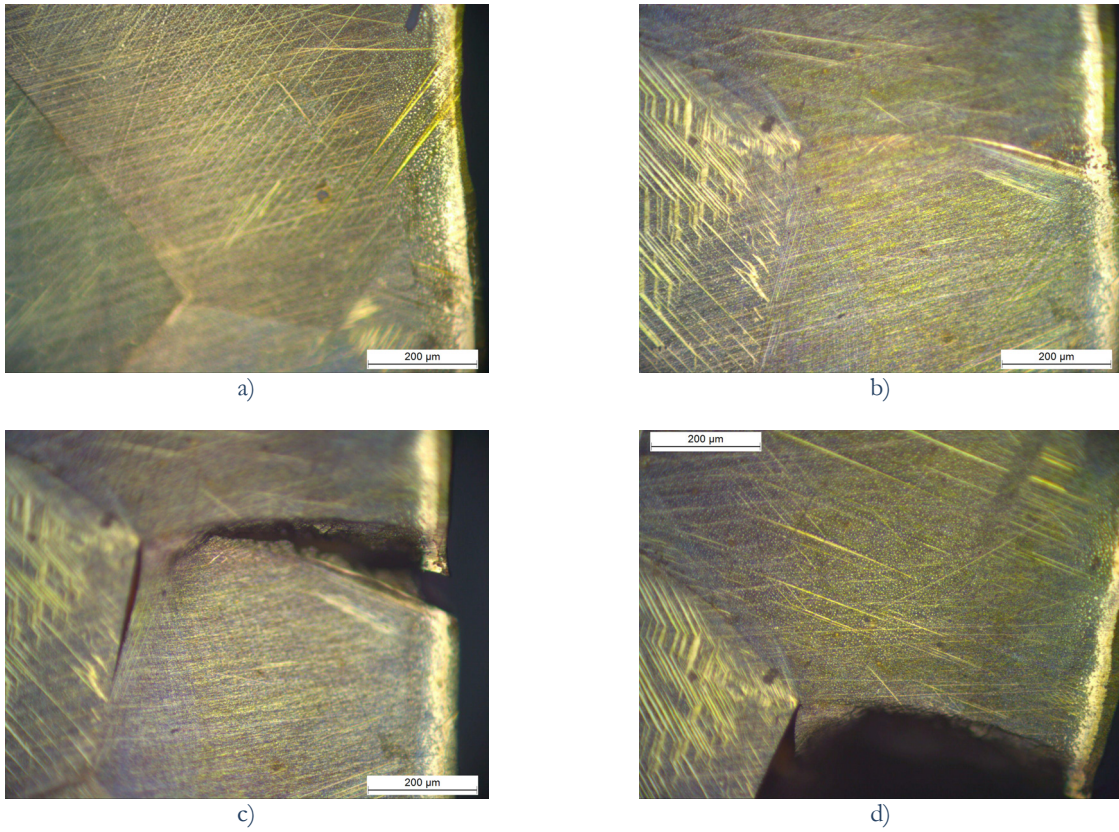


Figure 4: Fracture initiation zone: a) $\epsilon_{eng} = 0\%$, b) $\epsilon_{eng} = 5\%$, c) $\epsilon_{eng} = 10\%$, d) $\epsilon_{eng} = 14\%$ (failure).

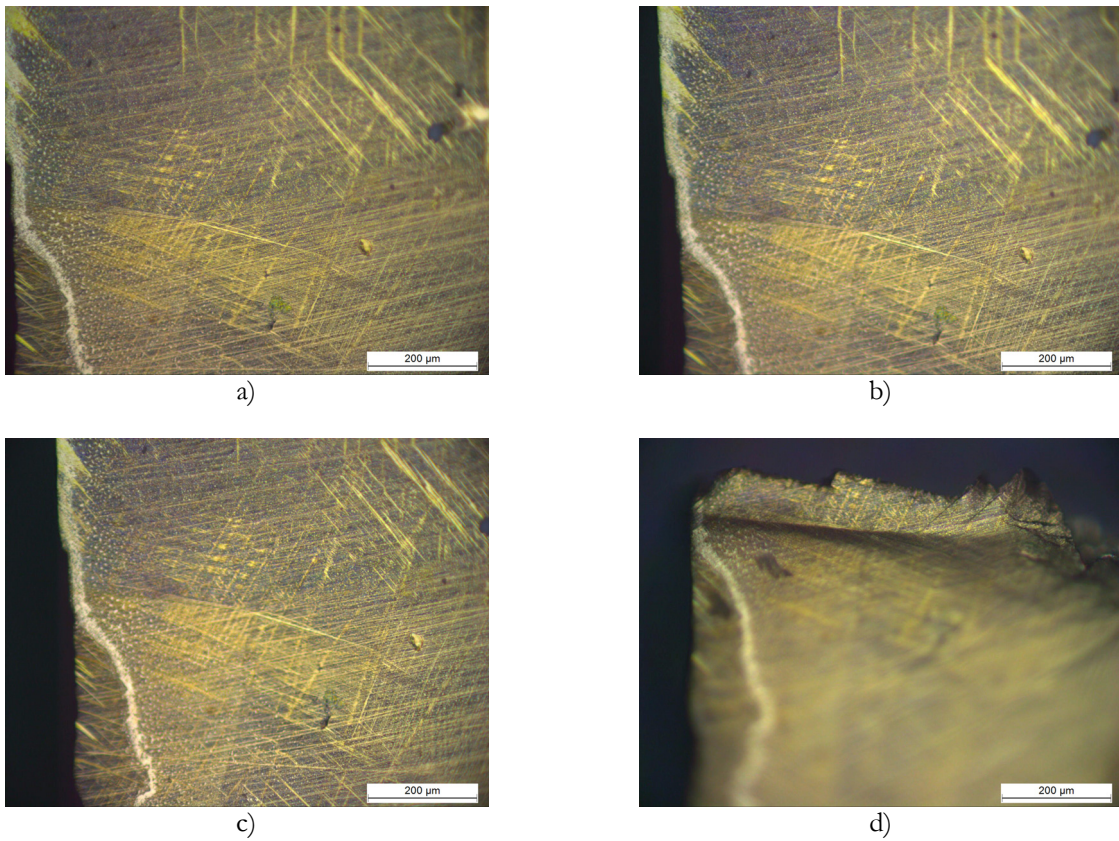


Figure 5: Fracture ending zone: a) $\epsilon_{eng} = 0\%$, b) $\epsilon_{eng} = 5\%$, c) $\epsilon_{eng} = 10\%$, d) $\epsilon_{eng} = 14\%$ (failure).

Fracture surfaces are characterized by a brittle morphology, as the intergranular cleavage shown in Fig.7a, which confirms the path observed on the lateral surface (Fig. 4c, d). According to the LOM damaging micromechanisms analysis and to SEM fracture surface analysis, grains decohesion seems to be main damaging micromechanisms. Inclusions presence implies the initiation of secondary microcracks (Fig. 7b), probably due to the same mechanism which characterizes the grain decohesion.

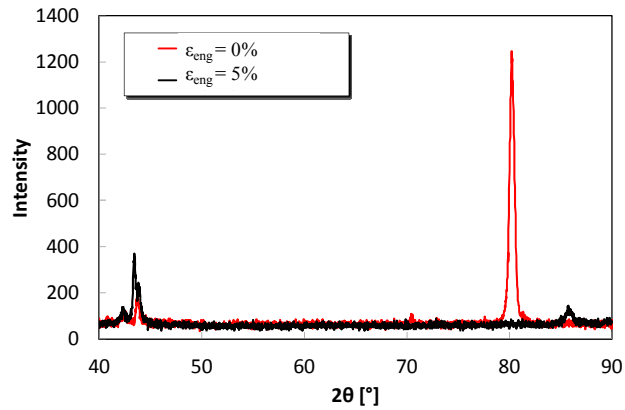


Figure 6: Diffraction spectra.

In the following photos, the “ending fracture zone”, corresponding to the highest deformation values (Fig. 5d), ductile fracture micromechanisms are shown (Fig 8). Two ductile morphologies are observed in Fig. 8 (respectively indicated by arrows with letters A and B). Morphology in A is characterized by an oriented plastic deformation, while morphology in B is characterized by an unoriented deformation.

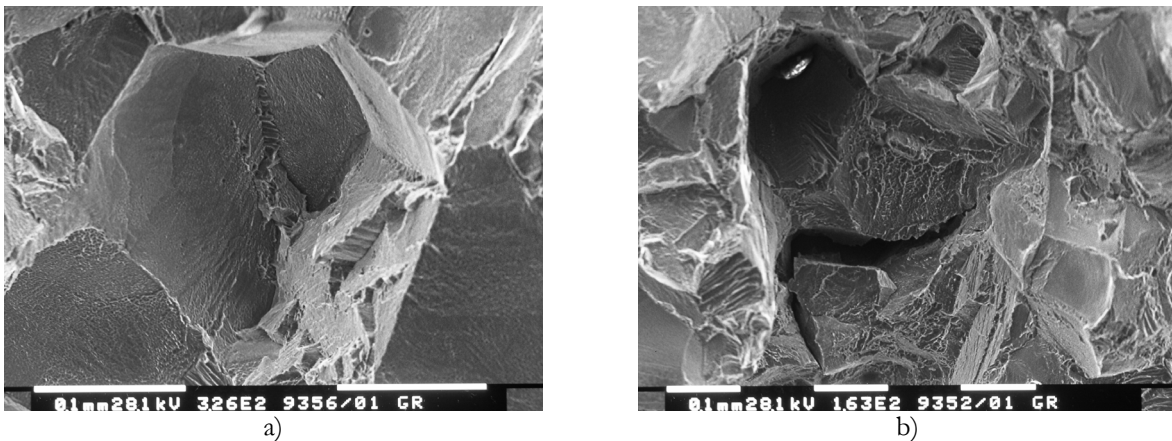


Figure 7: Fracture surface: a) intergranular cleavage, b) secondary crack in presence of inclusion.

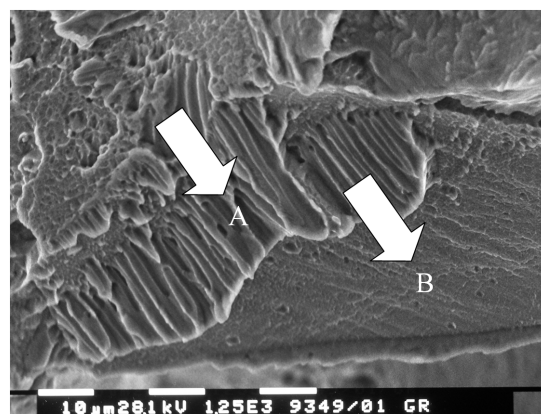


Figure 8: Fracture surface in the ending zone (as Fig. 5d)



Higher magnifications SEM observations (Fig. 9a and b) allow to confirm the ductile morphology of the fracture surface shown in Fig. 8.

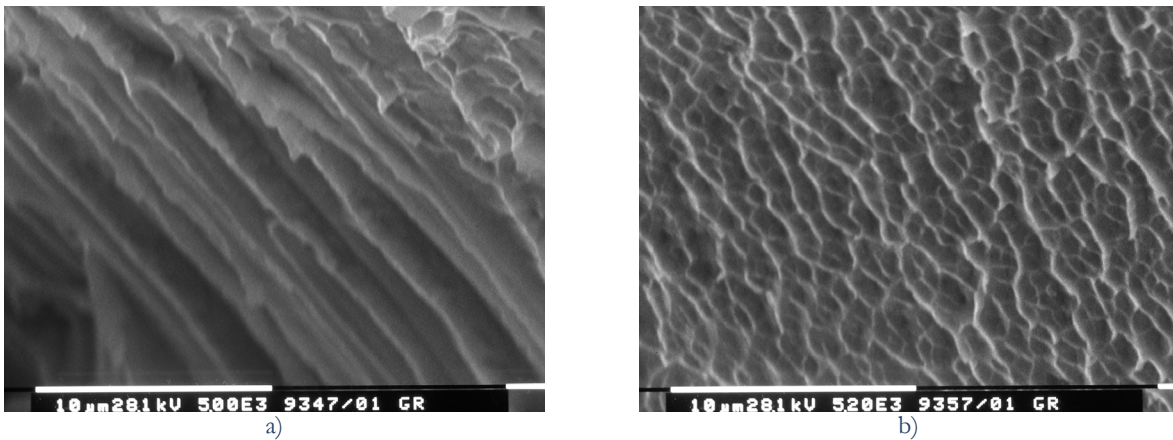


Figure 9: Fracture surface with high deformation: a) morphology of zone A of Fig. 8, b) morphology of zone B of Fig. 8.

CONCLUSIONS

In this work, the main crack initiation and propagation micromechanisms during tensile tests performed on a CuZnAl SMA was analyzed in correlation of electrochemical behaviour, microstructure etching and microstructure transition evidences from X-ray analyses. According to the experimental results, the following conclusions can be summarized as follows:

- Cracks initiate at grain boundaries due both to high deformation values and to phases transitions;
- Memory effect is not only due to phases transitions, but also to the unchanging of numbers of grains boundary;
- The main fracture surface morphology is brittle and is characterized by intergranular cleavage;
- Corresponding to the highest deformation values (“ending fracture zone”) the main damaging micromechanism is ductile.

REFERENCES

- [1] K. Otsuka, X. Ren, Progress in Materials Science (2005) 511.
- [2] Y. Dong, Z. Boming, L. Jun, Materials Science and Engineering A, 485 (2008) 243.
- [3] B. Chen, C. Liang, D. Fu, J. Mater. Sci. Technology, 21(2) (2005) 226.
- [4] Y. Liu, G.S. Tan, Intermetallics, 8 (2000) 1385.
- [5] P. Arneodo Larochette, M. Ahlers, Materials Science and Engineering, A361 (2003) 249.
- [6] N. Kayali, S. Ozgen, O. Adiguzel, Journal of Materials Processing Technology, 101 (2000) 245.
- [7] J.X. Zhang, Y.F. Zheng, L.C. Zhao, Acta mater., 47(7) (1999) 2125.
- [8] PowderCell 2.3—Pulverdiffraktogramme aus Einkristalldaten und Anpassung experimenteller Beugungsaufnahmen, in http://www.bam.de/de/service/publikationen/powder_cell.htm.